Applied Materials Today 26 (2022) 101263

Contents lists available at ScienceDirect

Applied Materials Today

journal homepage: www.elsevier.com/locate/apmt

Engineering of domain wall propagation in magnetic microwires with graded magnetic anisotropy

P. Corte-León[a,b], V. Zhukova[a,b], J.M. Blanco[b], A. Chizhik[a], M. Ipatov[a,b], J. Gonzalez[a], A. Fert[a,c], A. Alonso[d], A. Zhukov[a,b,e,*]

[a] Department of Advanced Polymers and Materials, Physics, Chemistry and Technology, Faculty of Chemistry, University of Basque Country, UPV/EHU, Paseo Manuel de Lardizabal 3, San Sebastian 20018, Spain
[b] Department of Applied Physics I, EIG, University of Basque Country, UPV/EHU, San Sebastian 20018, Spain
[c] Cnité Mixte de Physique, CNRS, Thales, Université Paris-Saclay, Palaiseau 91767, France
[d] CAF I+D S.L., C/ José Miguel Iturrioz, 26, Beasain 20200, Spain
[e] IKERBASQUE, Basque Foundation for Science, Bilbao 48011, Spain

ARTICLE INFO

Article history:
Received 13 July 2021
Revised 4 October 2021
Accepted 7 November 2021

Keywords:
Magnetic microwires
Domain wall propagation
Magnetic anisotropy
Annealing

ABSTRACT

We report on the influence of graded magnetic anisotropy designed by stress-annealing of magnetic microwire at variable annealing temperature on domain wall propagation. We found that the domain wall propagation in a medium with graded magnetic anisotropy is substantially nonuniform. Domain wall can be trapped in the microwire region with strong enough stress-annealing induced magnetic anisotropy. On the other hand, faster domain wall propagation and a decrease in the domain wall length are observed in the region with moderate stress-annealing induced magnetic anisotropy. Beneficial effect of stress-annealing on the domain wall dynamics is associated with the induced transverse magnetic anisotropy in the outer domain which affects the travelling domain wall in a similar way as application of transversal bias magnetic field. Observed decreasing of the half-width of the electromagnetic force (EMF) peak in stress-annealed microwires can be associated to the decreasing of the characteristic domain wall length.

1. Introduction

Studies of magnetic domain walls (DWs), which separate regions magnetized in opposite directions and the DWs propagation are in the focus of basic and applied interest because of variety of fundamental problems (*e.g.*, depinning of a DW from the pinning center through the magnetic quantum tunneling, magnetoelastic interaction of moving DW with the acoustic subsystem of the crystal, Cherenkov emission of sound by a moving DW, supersonic DW velocity, DW or skyrmion motion in nano/micro-wires with chiral exchange interactions,…) and exciting technological applications (*i.e.*, data storage or magnetic logics) [1–8].

In particular, it was shown that in soft magnetic materials with high shape anisotropy, like thin magnetic wires, the magnetic moments can be oriented along the long wire axis. Typically, under the effect of a reversed magnetic field in thin magnetic wires, one can observe the formation of reversed domains and the DW propagation [1,7,9,10]. Therefore, magnetic wires are one of the most convenient materials allowing DW dynamics studies. The basic aspects of the DW dynamics, such as the existence of a DW nucleation and propagation fields or the rate of change of DW velocity, v, with increasing the external field, H in terms of the DW mobility, S, have been established [7,9]. Great efforts have been made to control the single DW propagation using artificially created pinned centers by local notches, stray or local fields, or magnetostatic interaction or to understand the influence of magnetoelastic anisotropy [11–15]. In a number of promising applications, such as racetrack memories, magnetic logic or magnetic tags, the use of fast and controllable DW propagation has been proposed [4–6,9]. There are several materials that are quite attractive for such applications due to low magnetic anisotropy and yet high Curie temperature, such as submicrometric planar or cylindrical nanowires from permalloy or amorphous cylindrical submicrometric or micrometric wires [1–6,9,10,16–18].

Amorphous perfectly cylindrical magnetic microwires with metallic nucleus diameters, from 185 nm up to 100 μm can be ob-

* Corresponding author at: Department of Advanced Polymers and Materials, Physics, Chemistry and Technology, Faculty of Chemistry, University of Basque Country, UPV/EHU, Pareo Manuel de Lardizabal 3, San Sebastian 20018, Spain.
E-mail addresses: albert.fert@cnrs-thales.fr (A. Fert), arkadi.joukov@ehu.es (A. Zhukov).

https://doi.org/10.1016/j.apmt.2021.101263

tained by the so-called modified Taylor-Ulitovsky technique allowing fast (several meters per minute) preparation of almost continuous (up to 10 km long) microwires coated with a thin flexible and biocompatible glass coating with improved anti-corrosive and mechanical properties [9,10,16–20]. The fabrication method, including the rapid melt quenching of a metallic nucleus surrounded by glass with a rather different thermal expansion coefficients, causes strong predominantly tensile internal stresses [15–17,19,20]. Such microwires with positive magnetostriction coefficient usually present perfectly squared hysteresis loops associated with the magnetization switching through a single and large Barkhausen jump between two remanent states with opposite magnetization [9,10,21,22]. As observed elsewhere, the magnetization switching in magnetic wires runs through the DW propagation, which starts from the microwire ends, where closure domains appear due to the demagnetizing field effect [9,10,22–25]. The other soft magnetic wires, such as Permalloy nanowires, are usually produced using a variety of preparation techniques such as electron beam lithography, sputtering or deposition [1–5,11–13]. The high shape anisotropy of such nanowires ensures that magnetization alignment along the nanowires axis.

To compete with other technologies high speed of operation and, therefore, fast DWs propagation is required. The DW velocity, v, in nanowires of about 100 m/s is usually observed [4,5], while almost one order of magnitude higher v-values are reported in synthetic antiferromagnetic nanowires [26] and in amorphous microwires [9,10]. Such v-values can be further improved by various methods, involving either application of transverse magnetic field [9,27], ailoring of magnetoelastic anisotropy [9,28], or design of the magnetic anisotropy using appropriate post-processing [9,29].

For the proposed applications, it will be necessary to inject, controllably move and trap single or several DWs [1–5,9]. Therefore, several techniques, like local magnetic field, artificially created defects (notches or pads) or controlled DW collision, which served as DW pinning, annihilation injection sources are proposed [30–33]. Creation of structural irregularities (notches or protrusions) is demonstrated as an effective method for DW dynamics control either by pinning or DW injection in nanowires [11,12,30]. The position of a DW in a nanowire structure can be controlled by an intentionally fabricated notch or injected in a pad [11,12,30]. However, very few experimental results have been published on the effect of artificially created defects in amorphous microwires, which usually demonstrate much faster DW dynamics [34]. An artificial source of DW injection has been created by local stress-annealing [34].

Instead, braking or trapping of propagating DWs in a given position by a local antiparallel magnetic field in magnetic microwire is reported [35]. On the other hand, DWs can be injected into magnetic microwires either by a local magnetic field [36], or even by an opposite magnetic field, when an artificial source of DW injection is created by local stress-annealing [34]. Additionally, stress-annealing is an effective method for tuning of magnetic anisotropy of magnetic microwires [29,37]. Stress annealing of Fe-rich magnetic microwires allows the induction of transverse (with respect to the long wire axis) magnetic anisotropy [37], which affects the DW dynamics similarly to the application of a transverse bias magnetic field, allowing an increase in the DW mobility and a decrease in its length [29]. The peculiarity of stress-annealing induced anisotropy is that it essentially depends on the stress-annealing conditions: annealing temperature, time and stress applied during the annealing and can be partially annealed out by subsequent furnace annealing [29,38]. Accordingly, recently we showed that stress-annealing at fixed stress and variable annealing temperature allows creating magnetic microwire with graded magnetic anisotropy. The microwire annealed at variable temperature presents graded magnetic properties: different hysteresis loops and, hence, coercivity, H_c and squareness ratio, M_r/M_o, along the microwire [34].

As described elsewhere[1,39,40], in viscous regime the magnetic field, H, dependence of DW velocity, v, below the Walker breakdown field, H_W, in an infinite medium with constant magnetization at any point is well described in terms of DW mobility, S as:

$$v = S(H - H_0) \tag{1}$$

where H_0 is the critical propagation field.

Therefore, the DW dynamics in a medium with graded magnetic anisotropy is expected to be affected by magnetization distribution.

Accordingly, in this work we present a detailed study of the DW dynamics in a Fe-rich amorphous microwire with a graded magnetic anisotropy induced in the microwire by a specially designed thermal treatment consisting of stress-annealing at variable temperature.

2. Experimental details

We studied the most typical Fe-rich glass-coated microwire: $Fe_{75}B_9Si_{12}C_4$ microwires (metallic nucleus diameter $d = 15.2$ μm, total diameter $D = 17.2$ μm) with positive magnetostriction coefficient, λ_s, (38×10^{-6}) [41], prepared by the Taylor-Ulitovsky technique [16–18]. This technique allows preparation of up to few km long rather homogeneous and continuous microwires at the same quenching conditions. A piece of such a microwire with a length of about 24 cm was used for research. Part of such a sample was placed in a conventional furnace and annealed under tensile stress. Tensile stress, $\sigma \approx 760$ MPa, during annealing was created by a mechanical load attached to one end of the sample. Thus, part of the sample outside the furnace was simply loaded and unloaded, but part of the sample inside the furnace was subjected to stress annealing. The σ -value within the metallic nucleus was evaluated considering different Young moduli of the metal (E_2) and the glass (E_1), and the cross sections of the metallic nucleus and glass coating, as described elsewhere [37,38,43].

The temperature, T_{ann}, inside the furnace was set to 350 °C. Such T_{ann} was selected considering that the onset of crystallization in $Fe_{75}B_9Si_{12}C_4$ microwire is observed at about 520 °C [43]. Therefore, T_{ann} was selected to avoid the crystallization.

Accordingly, part of the sample was subjected to annealing at variable temperature, while part of the sample outside the furnace was not annealed. There is a zone inside the furnace where the temperature was constant. However, from the end of the furnace to the constant temperature zone, there is a zone temperature gradient zone.

The temperature, T, distribution from the furnace end to the zone with constant temperature was evaluated using the commercial (NiCr-Ni) thermocouple as follows: first, the desired furnace temperature was set ($T = 350$ °C). After stabilizing the temperature in the central zone of the furnace, the temperature distribution was measured by moving the thermocouple inside the furnace at the same location as the microwire sample during annealing. The temperature was measured every 5 mm. The accuracy of the temperature measurement in each point is ± 0.25 % (up to 1100 °C), the thermocouple diameter is 3 mm. During annealing, a microwire sample was placed in the furnace in a zone with a calibrated temperature distribution.As can be observed from Fig. 1, T variation from 80 °C up to 350 °C is observed from the furnace end up to the zone with constant T.

Accordingly, the microwire inserted into the furnace with the T set at 350 °C under tensile stress was subjected to stress annealing. However, a part of the microwire between the furnace end and the

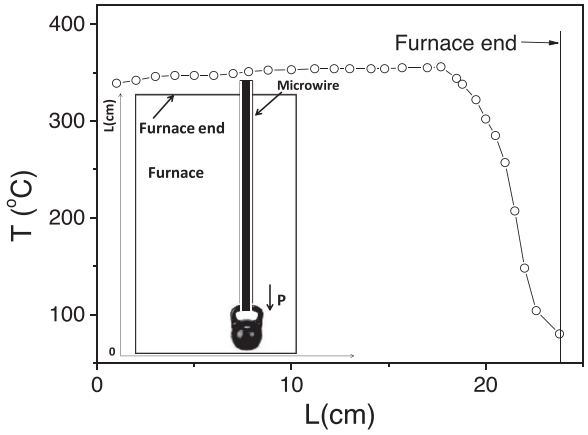

Fig. 1. Temperature distribution inside the furnace (with scheme of the microwire placed inside the furnace).

zone with T = const is subjected to stress annealing at a variable temperature.

Annealing was carried out in air: one of the advantages of glass-coated microwires is that an insulating and continuous glass coating can serve as protection against oxidation.

The hysteresis loops were evaluated using the fluxmetric method, previously used for characterization of magnetically soft microwires and described in details [42]. A thin (about 8 mm of diameter) 12 cm long solenoid creates a rather uniform axial magnetic field in the region where a sample of about 8 cm long is inserted [32]. The hysteresis loop of as-prepared sample was measured using 20 mm long pick-up coil. The fluxmetric method allows the measurement of hysteresis loops approximately up to $H \approx 3$ kA/m. For higher H measurements (required for the samples with strong transverse magnetic anisotropy) we used Quantum Design magnetometer (PPMS).

We present the normalized magnetization M/M_0 versus magnetic field H, where M is the magnetic moment at a given magnetic field and M_0 is the magnetic moment of the sample at the maximum magnetic field amplitude H_{max}. As-prepared microwire presents perfectly rectangular hysteresis loop, typically reported for Fe-rich amorphous microwires with $H_c \approx$ 55 A/m and $M_r/M_0 \approx 0.96$ (see Fig. 2a).

A short (2 mm long) pick-up coil was used to characterize the stress-annealed at variable T microwires which can show rather different hysteresis loops for different sections of the microwire. Such setup allowed us to measure the hysteresis loops of different sections of the microwire by moving it along the short pick-up coil.

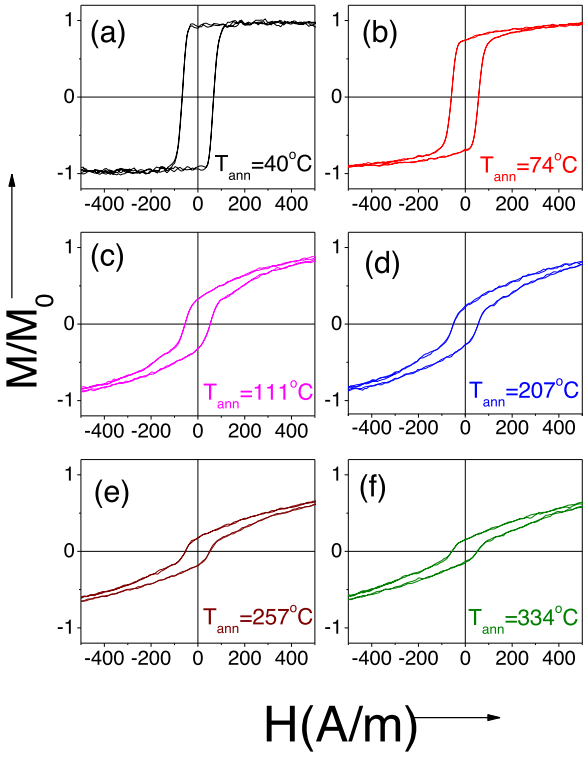

Fig. 3. Hysteresis loops of $Fe_{75}B_9Si_{12}C_4$ microwires stress-annealed at variable T_{ann} measured by short pick-up coil.

The DW velocity has been evaluated using the Sixtus-Tonks-like experiment previously successfully employed for DW dynamics studies in magnetic microwires [9,14,15,24]. The microwire has been placed inside the long solenoid creating magnetic field, H. One sample end is placed outside the magnetizing solenoid to ensure the DW propagation from the opposite wire end [9,14,15]. Three pick-up coils coaxially placed inside the solenoid, surrounding the sample and separated by the same distance, have been used for the DW velocity evaluation. Such experimental scheme allows avoiding exaggerated DW velocity values related to injection of additional DWs at high enough H-values [9,15].

The DW velocity, v, can be estimated from the time difference, Δt, in the electromotive force, EMF, peaks induced by the travelling DW in the pick-up coils, separated by the distance, l, as

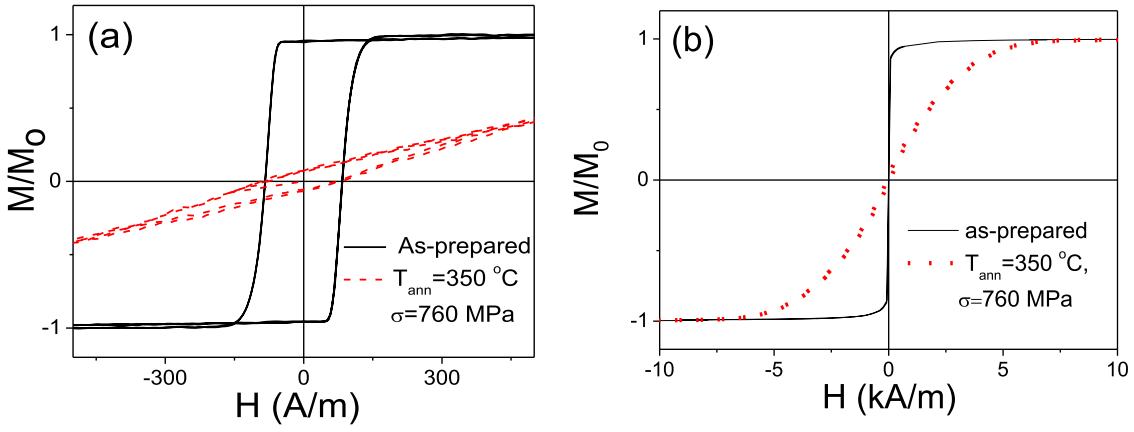

Fig. 2. Effect of stress-annealing on hysteresis loops of studied microwire measured at low field (a) and high field (b) range.

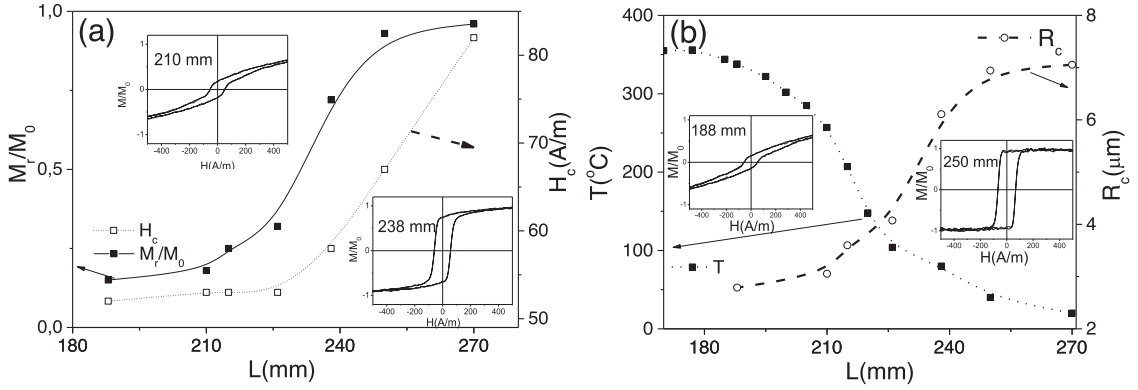

Fig. 4. M_r/M_0, H_c (a) and R_c (b) dependencies on L. The local hysteresis loops recorded at different L are provided in the insets.

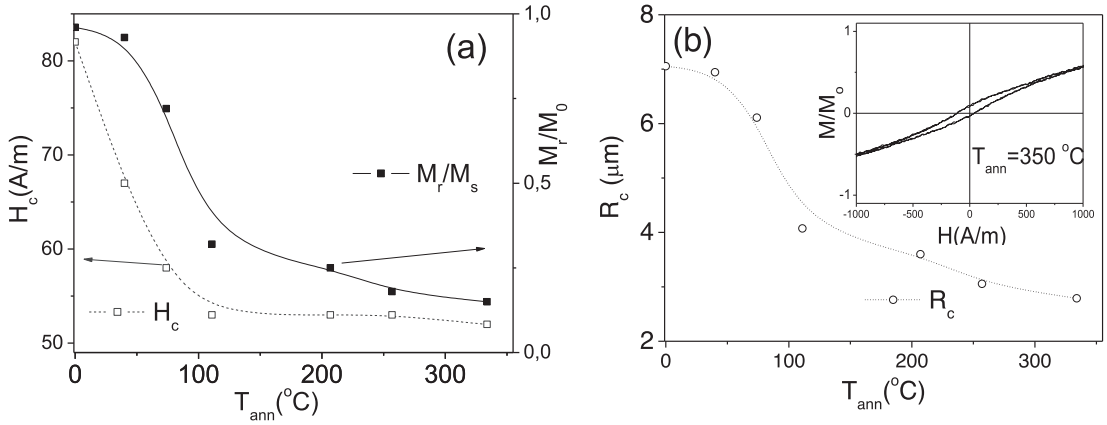

Fig. 5. M_r/M_0, H_c (a) and R_c (b) dependencies on T_{ann}. The local (L = 157 mm) hysteresis loop of the sample stress-annealed at T_{ann} = 350 °C is provided in the inset of Fig. 5b.

[9,14,15,44]:

$$v = \frac{l}{\Delta t} \tag{2}$$

The surface magnetization reversal process in the microwire has been studied by the longitudinal magneto-optical Kerr effect (MOKE) [45]. A polarized light of He–Ne laser was reflected from the surface of the wire to the detector. The laser beam diameter in the MOKE technique was of 0.8 mm. An axial magnetic field, H, has been produced by a pair of Helmholtz coils. The rotation of the angle of the light polarization reflected form the surface was proportional to the magnetization, which was parallel to the plane of the light and the microwire axis. The light reflected from the cylindrical surface of the wire forms a conical surface. As described elsewhere [45], to avoid a distortion of the magneto-optical signal related to the reflection from the non-planar surface, the part of light which corresponds to a small area of the wire surface was cut by the diaphragm and the lenses. In consequence, the curvature of this area is estimated to be about 3º. The metallic nucleus diameter was d = 15.2 μm. Taking into account that the spot size of the laser beam is about 1 mm, the area probed by the MOKE set-up can be estimated as about 10^{-3} mm^2. To study the distribution of the magnetic properties along the microwire length, the light beam was shifted along the microwire.

3. Experimental results and discussion

As mentioned above, as-prepared microwires presented rectangular hysteresis loops (see Fig. 2a). Rather different hysteresis loop is observed in the stress-annealed at T_{ann}= 350 °C sample annealed in the zone with T=const: a low field hysteresis loop presents completely different character with inclined hysteresis loop and rather low $M_r/M_0 \approx 0.08$. A macroscopic transverse anisotropy with magnetic anisotropy field, $H_k \approx 5$ kA/m can be easily appreciated from comparison of the hysteresis loop measured at high H (see Fig. 2b).

From previous publications related to the effect of stress-annealing on magnetic anisotropy of Fe-rich microwires, is known that the stress-annealing induced anisotropy depends on T_{ann} (at fixed t_{ann} and σ) [29,34,38]. Therefore, a modification of the hysteresis loops of the sample placed in the zone with variable T_{ann} (at fixed t_{ann} and σ) from the furnace end up to the zone with T_{ann} =const (see Fig. 1) is expected. Accordingly, as in Ref. [34], a gradual change in the local hysteresis loop (measured by the short pick-up coil) of the sample stress-annealed in the zone with variable T_{ann} is observed (see Fig. 3). Such microwire, stress-annealed at variable T_{ann} presents not only rather different hysteresis loops, but also variable squareness ratio, M_r/M_0, and coercivity, H_c, along the microwire length, L (see Fig. 4).

The most common model of domain structure of Fe-rich amorphous microwire comprises an inner axially magnetized core surrounded by an outer shell with radial magnetization orientation [23,46,47]. Therefore, observed $M_r/M_0(L)$ dependence can be used for evaluation of the inner axially magnetized core radius, R_c. Indeed, in the framework of core-shell domain structure model R_c can be evaluated from M_r/M_0 using the relation [23]:

$$R_c = R(M_r/M_0)^{1/2} \tag{3}$$

where R is the microwire radius.

Evaluated $R_c(L)$ dependence and its correlation with $T(L)$ profile are provided in Fig. 4b. Obtained $R_c(L)$, $M_r/M_0(L)$ and $H_c(L)$

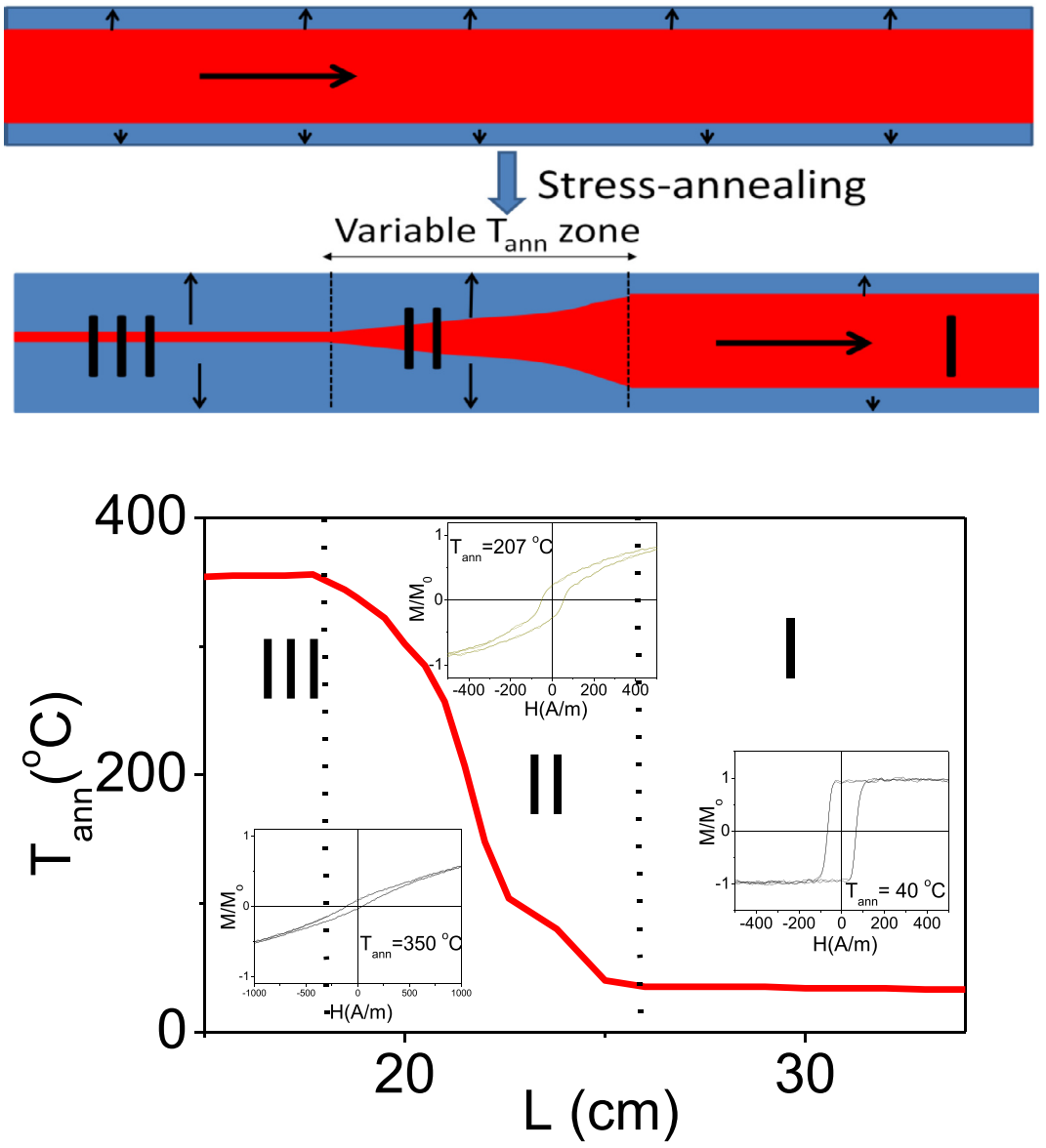

Fig. 6. Schematic picture of the graded magnetic anisotropy appearing as a continuous magnetic anisotropy gradient over the microwire length obtained by stress-annealing at variable T_{ann}.

dependencies and gradual change in hysteresis loop shape reflect graded magnetic anisotropy obtained by stress-annealing at variable T_{ann}. Taking into account a certain correlation of the $R_c(L)$, $M_r/M_0(L)$ and $H_c(L)$ dependencies with the $T(L)$ profile shown in Fig. 4b, the M_r/M_0, H_c and R_c (T_{ann}) dependencies have been evaluated (see Fig. 5a,b).

The observed $M_r/M_0(T_{ann})$, H_c (T_{ann}) and R_c (T_{ann}) dependencies demonstrate that the continuous magnetic anisotropy gradient along the microwire length evidenced from Figs. 3–5 must be attributed to the variable T_{ann} during the stress-annealing. Finally, the linear local hysteresis loop obtained at T_{ann} = 350 °C (in the microwire section stress-annealed at T= const on the $T(L)$ profile) is rather similar to the bulk hysteresis loop obtained for the same T_{ann} (see Fig. 2). Consequently, at fixed t_{ann} and σ, the stress-annealing induced transverse magnetic anisotropy becomes stronger with increasing T_{ann}.

In the present case, the graded magnetic anisotropy appears as a continuous spatial distribution of magnetic anisotropy gradient over the microwire length subjected to stress-annealing at variable T_{ann}. Taking into account the $R_c(T_{ann})$ and $R_c(L)$ dependencies, obtained graded anisotropy can be attributed to a gradual modification of the domain structure: an increase in the outer shell with transverse magnetic anisotropy in expense to a decrease in the inner core volume (see schematic picture in Fig. 6). Taking into account the modification in the character of local hysteresis loops along the sample with graded magnetic anisotropy, three different zones of the microwire can be identified.

The zone *I* corresponds to either as-prepared or stress-annealed microwire at low T_{ann} (approximately up to $T_{ann} \approx$ 74 °C) with almost perfectly rectangular hysteresis loops. The linear hysteresis loop, typical for microwires with transverse magnetic anisotropy is observed for the microwire section from zone *III* (stress-annealed at $T_{ann} \geq$ 334 °C). In the part of the microwire from zone *II*, we can assume a superposition of two types of magnetic anisotropy: transverse magnetic anisotropy, characterized by a rather low squareness ratio, and axial magnetic anisotropy, characterized by a sharp magnetization jump (74 °C$\leq T_{ann} \leq$ 334 °C) (see Fig. 6).

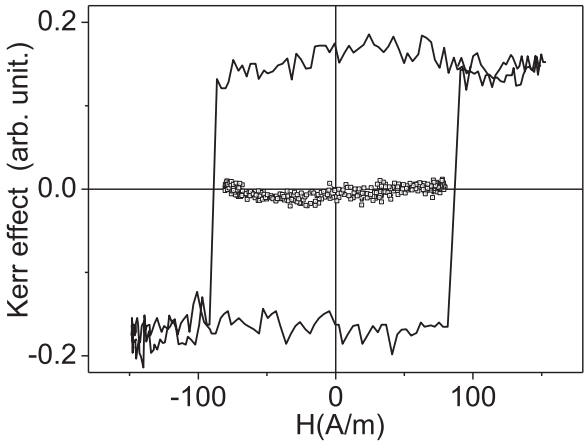

Fig. 7. Complete and minor hysteresis loops in zone *I*.

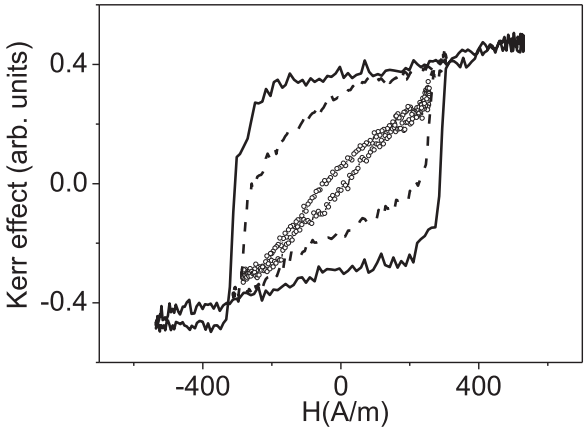

Fig. 8. Complete and minor hysteresis loops in zone *III*.

Such graded anisotropy, obtained by stress-annealing with variable T_{ann}, can be further tuned modifying the stress annealing conditions, *e.g.*, for a given T gradient, the magnetic anisotropy can be modified by t_{ann} and σ.

Transverse character of magnetic anisotropy in the surface of the microwires is indirectly confirmed by a remarkable giant magnetoimpedance effect improvement observed after stress-annealing of Fe-rich microwires [29,43].

Studies of surface magnetization reversal using MOKE technique can provide further details on the domain structure modification upon stress-annealing.

The complete and minor hysteresis loops from zones *I* and *III* of the microwire obtained by MOKE are shown in Figs. 7, 8.

The hysteresis loop shown in Fig. 7 corresponds to the portion of microwire with almost perfectly rectangular hysteresis (zone *I*). The rectangular shape of the MOKE hysteresis loop and the absence of the minor loop indicate the presence of magnetic bistability in this zone. In this case the MOKE hysteresis loops are rather similar to local hysteresis loops obtained by the fluxmetric method.

The complete MOKE hysteresis loop (Fig. 8, solid line) of the microwire from zone *III* can be interpreted as consisting of an axial magnetization jump and the magnetization rotation. The MOKE

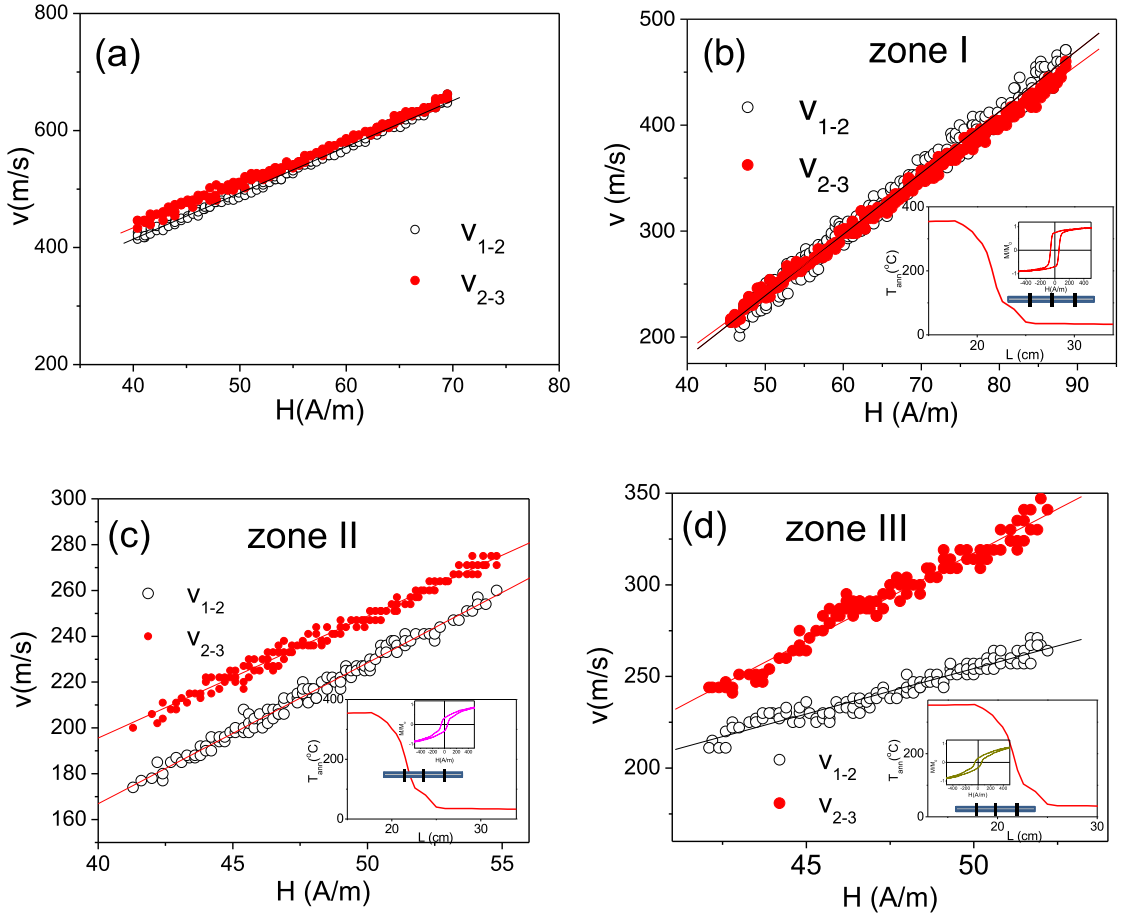

Fig. 9. *v(H)* dependencies of as-prepared (a) and stress-annealed at variable T_{ann} microwire (b–d) - when the sample with stronger transverse magnetic anisotropy is gradually inserted into the Sixtus-Tonks set-up.

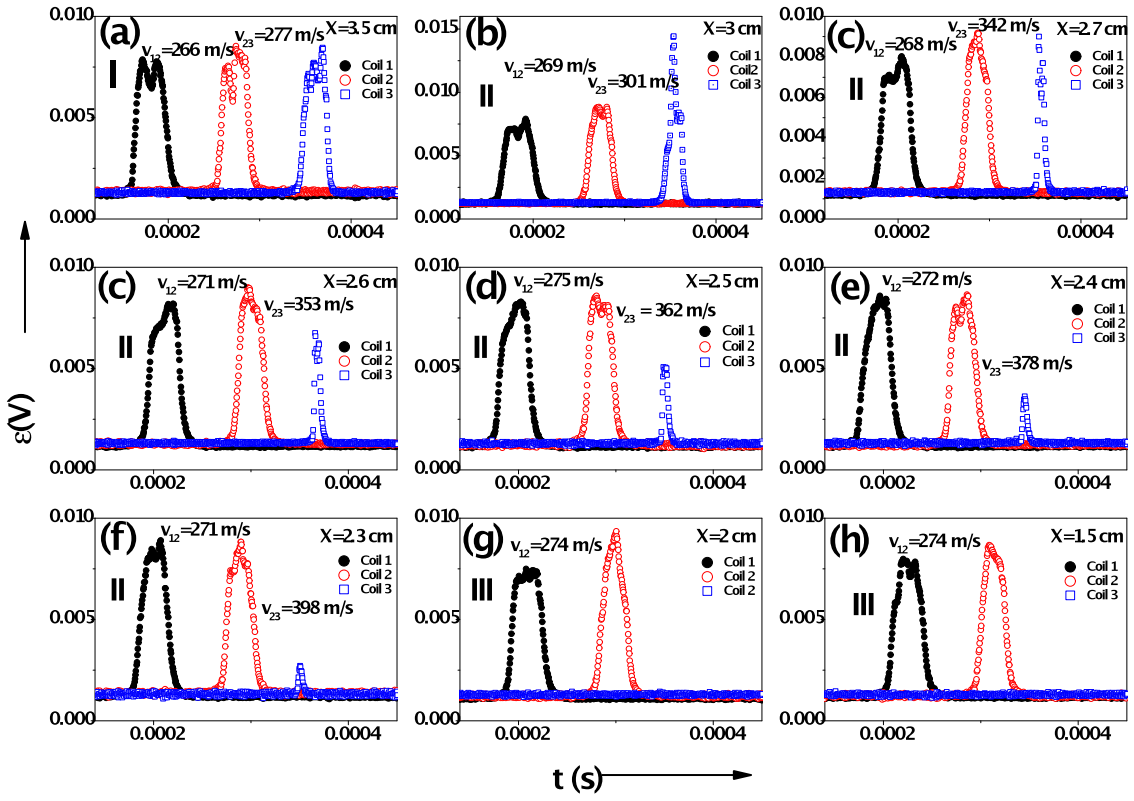

Fig. 10. The *EMF* peaks induced by the magnetization change in the pick-up coils in stress-annealed at variable T_{ann} microwire from zones *I* (a); *II* (b-f) and *III* (g, h) when the sample is inserted into the measuring system from the microwire end with rectangular hysteresis loop. Schematic picture of the DW propagation is provided in (i).

loop is affected by the *H* – value: the magnetization rotation contribution is clearly observed for all *H*-values. However, the magnetization jump, observed in the minor MOKE loop at sufficiently high *H*-values (see Fig. 8, dashed line) disappears once *H* decreases below some critical value (Fig. 8, the line with points). Generally, MOKE hysteresis loops present similar features with local and bulk hysteresis loops recorded for the same stress-annealing conditions by fluxmetric method (see Figs. 2a, 3 and 5b).

Indeed, both hysteresis loops can be described in terms of superposition of magnetization rotation and magnetization jump. The essential difference between these hysteresis loops is that MOKE hysteresis loops present higher coercivity, H_{cm}, as-compared to local hysteresis loops. In terms of aforementioned interpretation of the origin of graded magnetic anisotropy and related domain structure modification, such difference can be explained considering that the inner axially magnetized core radius, R_c, of such microwire portion (stress-annealed at rather high T_{ann}) is much smaller than the metallic nucleus radius, *R* (see Fig. 5b). Therefore, to observe the magnetization reversal of the inner axially magnetized core in the surface layer (using the MOKE method), a much higher *H*-value may be required as- compared to the case of the as-prepared microwire, in which $R_c \approx R$ (see Fig. 5b).

Accordingly, the character of the MOKE hysteresis loops of stress-annealed samples from zone *III* can be explained considering the contribution of the helical structure in the surface and the superposition of magnetization rotation and magnetization jumps.

Previously, for the preparation of magnetic materials (*i.e.*, thin films) with a graded magnetic anisotropy, rather sophisticated techniques were used, including a change in the chemical composition during the deposition of thin films with subsequent annealing [48,49]. The obtained gradient magnetic anisotropy in thin films appears as a continuous magnetic anisotropy gradient over the film thickness. The generation of required spatial distribution of the magnetic anisotropy was also proposed for the engineering of DW dynamics by controllable nucleation and propagation of the reversed domains using model calculations [50]. However, continuous anisotropy profiles are proposed to realize in solid solutions with spatially varying composition [50].

As regarding the DW propagation, the DW velocity in the Walker model, *v*, is given by [27,39,40]:

$$v = \left(\frac{2\pi\gamma\Delta}{\alpha}\right)H \tag{4}$$

where γ is the gyromagnetic ratio, α is the magnetic damping parameter Δ - DW width. The only variable parameters in the expression (4) are Δ and *H*. Consequently, in a viscous regime, characterized by a linear *v(H)* dependence, the DW propagation with a uniform velocity is usually assumed if *H*= const.

However, the energy landscape of the DW and hence the DW width, Δ, can be modified by several methods, *i.e.*, by the application of transverse field [51], as well as by induced transverse magnetic anisotropy [9,29]. Consequently, we can expect that the DW propagation in a microwire with graded magnetic anisotropy can be rather different.

Accordingly, DW dynamics has been evaluated for obtained microwire with graded magnetic anisotropy.

The comparison of *v(H)* dependencies of as-prepared and stress-annealed at variable T_{ann} microwire is shown in Fig. 9 b–d. The *v(H)* dependence of as-prepared sample is provided in Fig 9a, while the *v(H)* dependence shown in Fig. 9b corresponds to zone *I*. The difference between the Fig. 9b–d is that the sample with stronger transverse magnetic anisotropy is gradually inserted into the Sixtus-Tonks set-up. Accordingly, *v(H)* dependence shown in Figs. 9b,c is measured for the microwire zones *II* and *III*, respectively. As observed in Fig. 9a and b, DW velocity values obtained between the pair of pick-up coils 1-2 and 2-3, $v_{1\text{-}2}$ and $v_{2\text{-}3}$, respec-

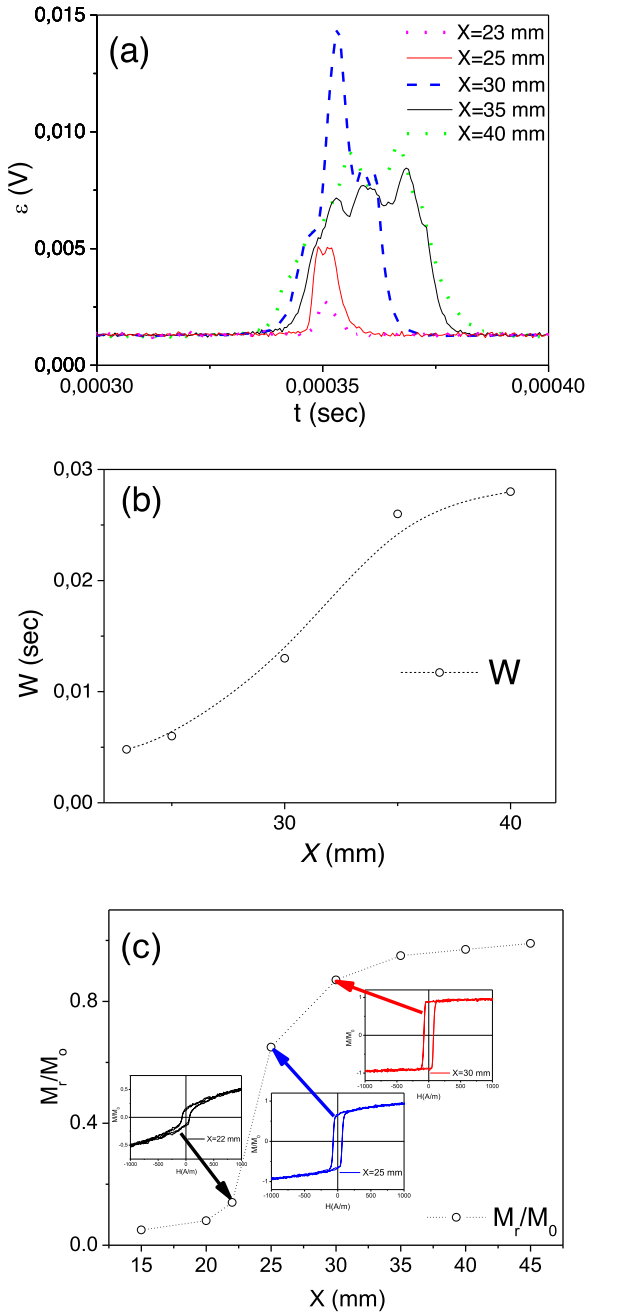

Fig. 11. Evolution of the *EMF* peak from the 3rd pick-up coil with *X* (a), half-width of the 3rd *EMF* peak as a function of *X* (b) and M_r/M_0 dependence with X (c).

tively, are almost identical. This means that in as-prepared sample as well as in the sample with weak stress-annealing induced magnetic anisotropy DW travels with a constant velocity at a given *H* -value.

Finally, $v_{1\text{-}2}$ and $v_{2\text{-}3}$ values become quite different. Such difference must be attributed to non-uniform DW propagation (v ≠const). As observed from Fig. 7c,d, as a rule $v_{2\text{-}3}$ values are considerably higher.

The sample section in which faster DW propagation is observed corresponds to the stronger transverse magnetic anisotropy. This result is consistent with recently reported influence of the stress-annealing induced magnetic anisotropy on DW dynamics. An improvement in DW velocity is attributed to the influence of the outer domain shell with transverse magnetic anisotropy (evidenced by R_c decrease observed in Fig. 5b upon T_{ann} increasing) associated to stress-annealing induced transverse magnetic anisotropy [29]. Such induced magnetic anisotropy of transverse origin is assumed to affect the DW dynamics in a similar way as the transverse magnetic field [9,29].

Additional information can be obtained from the *EMF* signals, ε, induced in the pick-up coils by the travelling DW [29]. In addition to the *v*-value (evaluated from Eq. (2)), the time ε dependence, $\varepsilon(t)$, can provide information on the uniformity of the DW velocity, the DW shape, and even on the cross section of the region where DW propagates [9,29,52,53].

Experimental results on $\varepsilon(t)$ dependencies recorded for different sections of studied sample are shown in Figs. 10 and 11.

Fig. 10 (a–h) are obtained for the case when the sample is gradually inserted from the zone *I* side into the measuring system consisting of 3 pick-up coils from the side of the 3-rd pick-up coil. Each Figure (a–h) is obtained when the opposite sample end at a different distance, *X*, is outside the solenoid end (see Fig. 10i). In this configuration, the singe DW depins and travels from the sample region (from the end placed inside the magnetizing solenoid), which presents the features of magnetic bistability and the stress-annealing induced anisotropy is either absent or rather small (see Fig. 10i). However, DW propagation takes place in the sample region affected by stress-annealing at variable T_{ann} (when the sample is inserted sufficiently inside the solenoid).

Consequently, the DW propagation is first measured for the zone *I*. Then, the sample from zones *II* and *III* step by step moves inside the measuring system (from the side of the 3rd pick-up coil). The $\varepsilon(t)$ dependencies observed for the microwire portion from the zone *I* are quite typical for the regular DW propagation with a uniform velocity: travelling DW passes successively through the first, second and third pick-up coils (see Fig. 10a). All the *EMF* peaks present quite similar amplitude, shape and separated by roughly the same Δt, indicating the single-DW propagation regime with DW travelling at constant velocity.

Different picture is observed when the microwire from the zone *II* reaches the 3rd pick-up coil (Fig. 10b): in such sample position the signal from the 3rd pick-up coil (in which the microwire from zone *II* is inserted) becomes much sharper. The *EMF* peak amplitude of the 3rd pick-up coil first becomes higher and then decreases when the sample further moves inside the measuring system (see Fig. 10c–f).

Such changes are evidenced by the evaluation of the peak appearing in 3rd pick-up coil and half-width (full width at half maximum), *W*, of the *EMF* signal with distance, *X*, shown in Fig. 11a,b. As clearly seen from Fig. 11a, 3rd peak becomes sharper when the sample zone with stronger stress-annealing induced anisotropy is inserted inside the 3rd pick-up coil.

This behavior is evidenced from *W(X)* dependence shown in Fig. 11b.

Additionally, the Δt between the 2nd and 3rd pick-up coils becomes smaller. This indicates that the DW of the sample from the zone *II* travels faster (as also evidenced from Fig. 9d).

Accordingly, such evolution of the 3rd *EMF* peak must be associated to a decrease in the characteristic DW length, δ, or/and to a modification in the DW velocity.

In the simplified case, when the characteristic DW δ, is small as-compared with the distance, *z*, from the coil turn to the DW position, the *EMF*, ε, generated in the pick-up coil turn is given by [29,54]:

$$\varepsilon(t) = -\frac{2\pi Q v}{c}\frac{R^2}{\left(z+R^2\right)^{3/2}} \tag{5}$$

where *c* is the speed of light, *R* is the radius of the coil turn, $v = -dz/dt$- domain wall velocity and *Q*- magnetic charge.

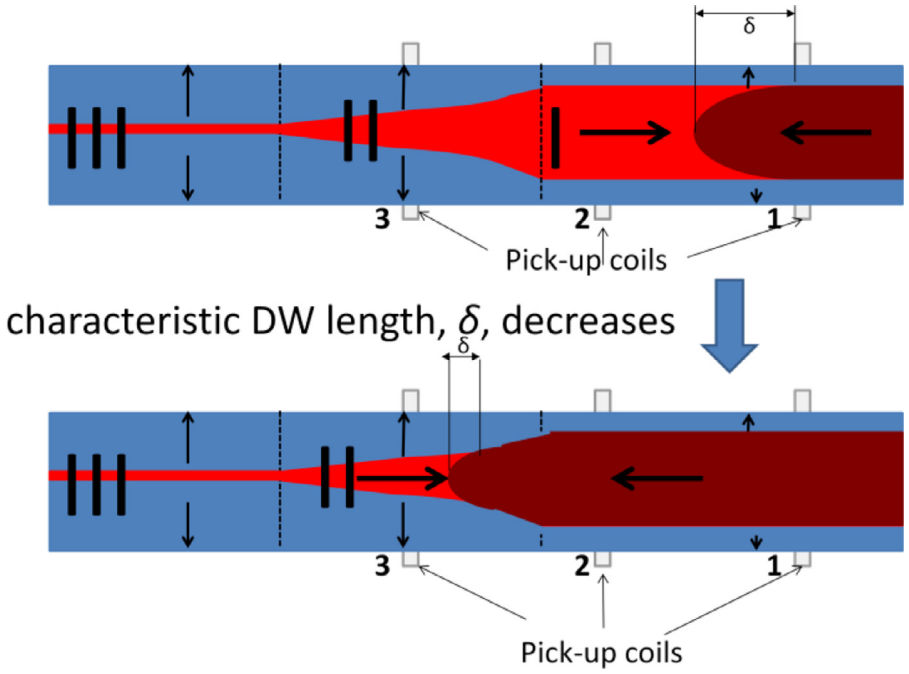

Fig. 12. Schematic picture illustrating the modification of the DW length in the zone with graded magnetic anisotropy.

We can compare the *EMF* signals detected by the 3rd pick-up coil if we consider the same coil parameters. In this case, such difference must be attributed to the change in *Qv* product. Accordingly, the *EMF* modification observed in Figs. 10 and 11 must be associated either to the different DW velocity, *v*, values, or the change in the magnetic charge, *Q*, given as [29]:

$$Q = 2M_rS \tag{6}$$

where *S* is the sample cross section and M_r – remanent magnetization.

Previously, these effects have been separated from comparison of evolution of *Qv* and *W* [29]. In the present case, studied DW propagation takes place in the sample zone with graded magnetic anisotropy, where M_r/M_0 gradually changes along the sample (see Fig. 11c). Therefore, strictly speaking, DW velocity observed in zone *III* (Fig. 9d) must be variable along the sample (*i.e.*, different in each point of the sample from zone *III*). For $H = 45$ A/m the ratio between the *v* -values between $v_{1\text{-}2}$ and $v_{2\text{-}3}$ is $v_{1\text{-}2}/v_{2\text{-}3} \approx 0.85$ (see Fig. 9d). On the other hand, the average remanence ratio taken from the Fig. 11c $M_r/M_{0(1\text{-}2)}$ / $M_r/M_{0(2\text{-}3)} \approx 2$. Accordingly, such simplified estimation gives $Q_{1\text{-}2}\ v_{1\text{-}2}$ / $Q_{2\text{-}3}\ v_{2\text{-}3} \approx 1.7$. Let us consider as $W_{1\text{-}2}$ and $W_{2\text{-}3}$ *W*-values for the zones *I* and *III*. Accordingly, the ratio $W_{1\text{-}2}/W_{2\text{-}3}$ evaluated from Fig. 11b gives an average value $W_{1\text{-}2}/W_{2\text{-}3}$ about 4.5. Therefore, observed difference in 3rd peak half-width cannot be explained only by different DW velocities in zones *I* and *III*.

Consequently, we can assume that the characteristic DW length, δ, decreases when the DW propagates in the zone with graded magnetic anisotropy as schematically shown in Fig. 12.

Such decrease in δ is related to both, a decrease in the cross section of the inner axially magnetized core in which the DW is located as well as by an increase in the magnetic anisotropy constant, *K*, due to stronger induced magnetic anisotropy. The δ –values are affected by the anisotropy constant, *K*: the reduced head-to-head domain wall length δ/d (*d* is the metallic nucleus diameter) changes from $\delta/d \approx 13.5$ for $K = 10^3$ J/m^3 to $\delta/d = 40$–50 for $K = 10^2$ J/m^3 [54]. On the other hand, even at fixed magnetic anisotropy the DW length is affected by the wire diameter [9,54]. Accordingly, the decrease in reduced head-to-head domain wall length in the sample portion subjected to stress-annealing at high enough T_{ann} (see Fig. 12) must be attributed to both decrease in the inner core radius and higher magnetic anisotropy in stress-annealed sample section.

As can be deduced from the above discussion, DWs in amorphous microwires are quite long: in contrast to nanowires, where δ is of the order of the wire diameter, *i.e.*, $\delta/d \sim 1$ – 2 [4], in amorphous Fe-rich microwires $\delta\ /d \sim 13.5$–50 [9,54]. This difference is primarily related to the low magnetic anisotropy of amorphous microwires as well as low contribution of the exchange energy for microwires with thicker dimensions.

Substantially non-abrupt DWs were detected from the analysis of *EMF*, ε, induced in the pick-up coil during DW propagation in Fe-rich microwires [54–56]. The micromagnetic origin of such long DWs is still unclear. Nevertheless, several attempts have been made to evaluate the DWs shape from the *EMF* signals induced in the pick-up coils, assuming cylindrical symmetry [56–58].

The DW shape with a narrow tail at one end and close to cylindrical at the other end was obtained from the *EMF* signal [56]. This DW shape allows the decrease in the magnetostatic energy by minimizing the surface area. On the other hand, conical [57], and planar [58], DWs in Fe-rich microwires have been proposed. The unusually high DW velocity observed in microwires can be explained considering that the normal DW velocity, v_n, can be up to two orders of magnitude lower that the axial DW velocity, *v*, (considering that v_n is related to the axial DW velocity by a factor R_c/δ).

Rather different behavior is observed if the sample is inserted into the measuring system from the opposite side. In this case the sample end subjected stress-annealing at variable T_{ann} (zones *III* and *II*) is placed inside the measuring system. The opposite sample end (zone *I*) which presents rectangular hysteresis loop is partially placed outside the magnetizing solenoid (see scheme in Fig. 13e). Therefore, the DW depinning must start from the samples region with strong stress-annealing induced anisotropy (zones *III* and *II*). At the initial stage (Fig. 13a) the only part of the sample presenting magnetization jump (zone *II*) is inserted between the 2nd and 3rd pick-up coils (see Fig. 13). In this case, the DW propagation is ob-

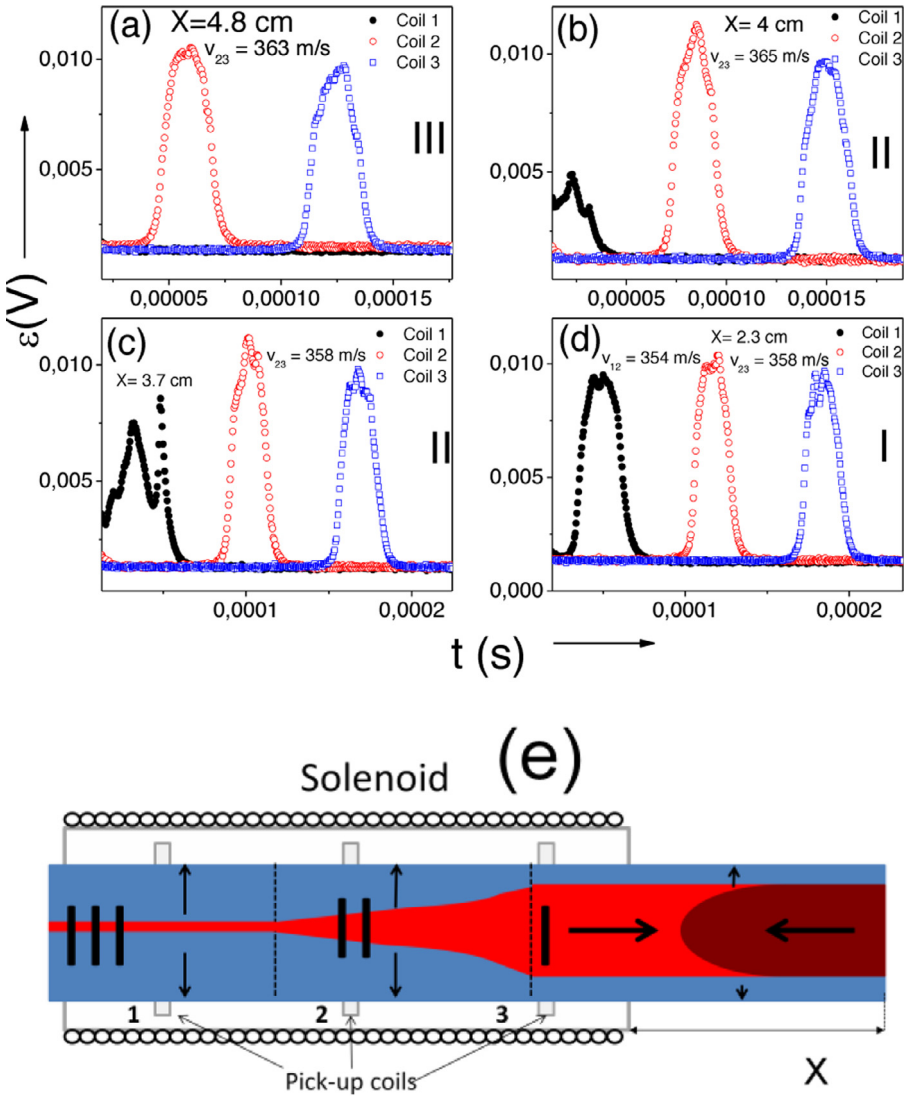

Fig. 13. The *EMF* peaks induced by the magnetization change in the pick-up coils in stress-annealed at variable T_{ann} microwire from zones *III* (a), *II* (b,c) and *I* (d) when the sample is inserted into the measuring system from the side stress-annealed at variable T_{ann}. Schematic picture of the DW propagation is provided in (e).

served only between the pick-up coils 2 and 3. Once the sample is inserted sufficiently inside the magnetized solenoid (*i.e.*, when the sample portion from zone *III* reaches the position of the 1st pick-up coil), the *EMF* peak in the first coil becomes visible. However, in this case the peak is rather wide and irregular (see Fig. 13b,c). Finally, when the sample region with rectangular hysteresis loop is inserted sufficiently deep inside the magnetizing solenoid, the *EMF* peaks sequence becomes similar to regular.

Accordingly, from the comparison of Figs. 11 and 13 we can deduce that the DW dynamics in microwires with graded magnetic anisotropy is substantially affected by the direction of the applied axial magnetic field. Such unidirectional character of DW dynamics can be suitable for magnetic logic applications [6].

Considering provided above experimental results, the magnetic field driven DW propagation in magnetic microwire with graded magnetic anisotropy obtained by stress-annealing at variable T_{ann} can be described as following:

As shown experimentally in various families of Fe-rich magnetic microwires [23,46,47,59,60], in as-prepared Fe-rich microwires with perfectly rectangular hysteresis loops at $H=0$ the domain structure consists of inner axially magnetized domain and closure domains at the ends surrounded by the outer domain shell (see Fig. 14 a). In as-prepared Fe-rich microwires radial magnetization orientation of the outer shell is experimentally observed [46,59].

Once the external magnetic field reaches the switching field, H_s, the magnetization switching through a single and large Barkhausen jump starts from the microwire ends, where closure domains appear due to the demagnetizing field effect (see Fig. 14a) [23,60]. Accordingly, once $H > H_s$, a single DW travels along the microwire (see Fig. 14b).

As evidenced from local hysteresis loops and evolution of M_r/M_0 with T_{ann} (Figs. 4–6), the volume of inner axially magnetized core decreases upon stress-annealing. As regarding the outer domain shell, circumferential magnetization orientation in outer domain shell is predicted from the character of magnetic field dependence of the Giant magnetoimpedance ratio [42,43], as shown in Fig. 14c.

As shown in Fig. 14c, the inner axially magnetized core radius in the microwire portion subjected to stress-annealing at high enough T_{ann} becomes smaller. Accordingly, in the sample portion subjected to stress-annealing at high enough T_{ann} the DW length decreasing is observed (see Fig. 14c).

The proposed method for modification of the axially magnetized core radius by stress-annealing with a temperature gradient can serve as an alternative to engineer the DW dynamics through

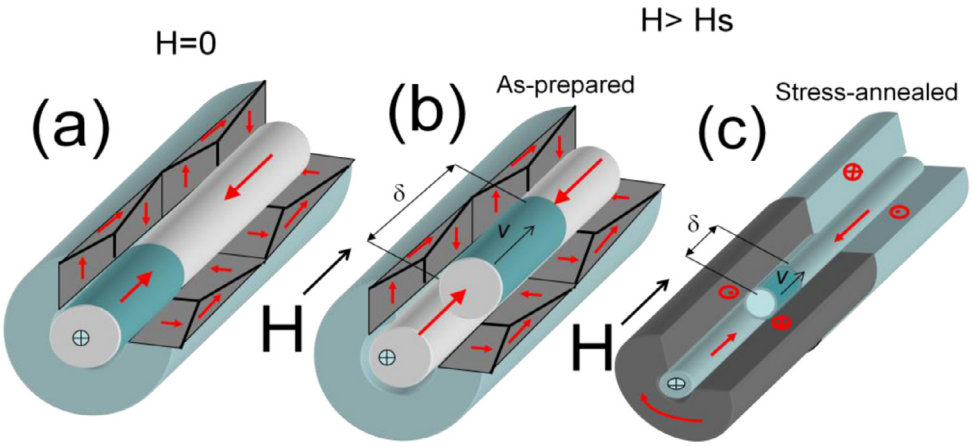

Fig. 14. Schematic picture of domain structure of as-prepared samples at $H = 0$ (a), $H>H_s$ (b) and stress-annealed sample portion at $H>H_s$(c).

different anisotropy characteristics in the same way as in multi-segmented nanowires synthesized by controlled electrodeposition [61]. However, the proposed method allows obtaining such properties in a much simpler way without the use of controlled electrodeposition.

The origin of observed stress-annealing anisotropy, presents partially reversible character [34,38], and was recently discussed considering either "back" stresses [38], or compositional and topological short-range ordering [38,62–64]. The topological short range ordering (also known as structural anisotropy) is associated with the angular distribution of the atomic bonds and small anisotropic structural rearrangements at elevated temperature [63,64].

Another factor that can affect the DW dynamics of stress-annealed at variable temperature microwires is that annealing can affect intrinsic properties such as damping. In most publications, no effect of stress annealing on the damping parameter was observed [65,66]. However, one of the damping mechanisms associated with small displacements of mobile defects can affect the local magnetic anisotropy and DW dynamics [67]. Therefore, the observed effect of graded magnetic anisotropy on DW dynamics can also be related to the effect of stress annealing on the damping parameter.

In the present case, upon annealing at fixed applied stress but at variable T_{ann} we are able to design a media with artificially modified inner core radius which serves as a gate for DW propagation in amorphous microwires. Such modification in the volume of the inner axially magnetized core allowed us to modify the DW dynamics or even to pin the propagating DW at desired region of microwire (see Fig. 10). Additionally, we propose rather simple way to design graded magnetic anisotropy in magnetic microwire by stress-annealing at variable T_{ann}.

4. Conclusion

We have proposed rather simple method to design graded magnetic anisotropy in magnetic microwire by stress-annealing at fixed applied stress and variable annealing temperature. A gradual modification of hysteresis loops consisting of variable squareness ratio and coercivity along the microwire length is achieved in microwires subjected to stress annealing with a temperature gradient. The obtained medium with an artificially modified inner axially magnetized core radius, which serves as a gate for DW propagation, allows engineering of DW dynamics in Fe-rich microwires by graded magnetic anisotropy. We found that the velocity of a single DW propagation in such media with graded magnetic anisotropy is essentially non-uniform, varying along the microwire. Additionally, in the microwire section with a sufficiently strong stress-annealing induced magnetic anisotropy, the DW can be trapped. On the other hand, a faster DW propagation and a decrease in the DW length are observed in the section with moderate graded stress-annealing induced magnetic anisotropy. The observed decrease in the half-width of the electromagnetic force (EMF) peak in stress-annealed microwires has been associated with a decrease in the characteristic domain wall length.

The beneficial effect of stress-annealing on the domain wall dynamics is associated with the induced transverse magnetic anisotropy in the outer domain shell, which affects the travelling domain wall in a way similar to the application of a transverse bias magnetic field.

The proposed method for engineering the DW dynamics through different anisotropy characteristics allows to combine the fast DW propagation characteristic for amorphous microwires with possibilities to control the DW dynamics.

The dependence of the DW dynamics on the applied magnetic field direction, found in a region with graded magnetic anisotropy, can be useful for magnetic DW logic applications.

Data availability

The raw/processed data required to reproduce these findings cannot be shared at this time as the data also forms part of an ongoing study.

Declaration of Competing Interest

The authors declare that they have no known competing financial interests or personal relationships that could have appeared to influence the work reported in this paper.

CRediT authorship contribution statement

P. Corte-León: Data curation, Writing – review & editing, Visualization, Investigation. **V. Zhukova:** Data curation, Resources, Visualization, Investigation, Methodology. **J.M. Blanco:** Data curation, Visualization. **A. Chizhik:** Data curation, Visualization. **M. Ipatov:** Data curation, Visualization, Methodology. **J. Gonzalez:** Resources, Funding acquisition. **A. Fert:** Writing – review & editing, Supervision. **A. Alonso:** Funding acquisition, Resources. **A. Zhukov:** Conceptualization, Supervision, Writing – original draft, Writing – review & editing, Investigation, Funding acquisition.

Acknowledgments

This work was supported by the Spanish MCIU, under PGC2018-099530-B-C31 (MCIU/AEI/FEDER, UE), by the Government of the Basque Country, under PIBA 2018-44, PUE_2021_1_0009 and Elkartek (CEMAP and AVANSITE) projects, and by the University of Basque Country, under the scheme of "Ayuda a Grupos Consolidados" (Ref.: GIU18/192) and COLAB20/15 project. The authors are thankful for the technical and human support provided by SGIker of UPV/EHU (Medidas Magnéticas Gipuzkoa) and European funding (ERDF and ESF).

References

[1] T. Ono, H. Miyajima, K. Shigeto, K. Mibu, N. Hosoito, T. Shinjo, Propagation of a magnetic domain wall in a submicrometer magnetic wire, Science 284 (1999) 468.
[2] V.G. Bar'yakhtar, B.A. Ivanov, M.V. Chetkin, Dynamics of domain walls in weak ferromagnets, Sov. Phys. Uspekhi 28 (1985) 563–588.
[3] J. Xia, X. Zhang, M. Yan, W. Zhao, Y. Zhou, Spin-Cherenkov effect in a magnetic nanostrip with interfacial dzyaloshinskii-moriya interaction, Sci. Rep. 6 (2016) 25189, doi:10.1038/srep25189.
[4] S.S.P. Parkin, M. Hayashi, L. Thomas, Magnetic domain-wall racetrack memory, Science 320 (2008) 190.
[5] G.S.D. Beach, C. Nistor, C. Knutson, M. Tsoi, J.L. Erskine, Dynamics of field-driven domain-wall propagation in ferromagnetic nanowires, Nat. Mater. 4 (2005) 741–744, doi:10.1038/nmat1477.
[6] D.A. Allwood, G. Xiong, C.C. Faulkner, D. Atkinson, D. Petit, R.P. Cowburn, Magnetic domain-wall logic, Science 309 (2005) 1688.
[7] A. Thiaville, Y. Nakatani, Domain-wall dynamics in nanowires and nanostrips. In: B. Hillebrands, A Thiaville (eds) Spin Dynamics in Confined Magnetic Structures III. Topics in Applied Physics, vol 101. Springer, Berlin, Heidelberg, doi:10.1007/10938171_5.
[8] C. Ma, X. Zhang, J. Xia, M. Ezawa, W. Jiang, T. Ono, S.N. Piramanayagam, A. Morisako, Y. Zhou, X. Liu, Electric field-induced creation and directional motion of domain walls and skyrmion bubbles, Nano Lett. 19 (1) (2019) 353–361.
[9] V. Zhukova, P. Corte-Leon, L. González-Legarreta, A. Talaat, J.M. Blanco, M. Ipatov, J. Olivera, A. Zhukov, Review of domain wall dynamics engineering in magnetic microwires, Nanomaterials 10 (2020) 2407.
[10] V. Zhukova, A. Zhukov, J.M. Blanco, J. Gonzalez, B.K. Ponomarev, Switching field fluctuations in a glass coated Fe-rich amorphous microwire, J. Magn. Magn. Mater. 249/1-2 (2002) 131–135.
[11] L.K. Bogart, D. Atkinson, K. O'Shea, D. McGrouther, S. McVitie, Dependence of domain wall pinning potential landscapes on domain wall chirality and pinning site geometry in planar nanowires, Phys. Rev. B 79 (2009) 054414.
[12] D. Djuhana, H.G. Piao, S.H. Lee, D.H. Kim, S.M. Ahn, S.B. Choe, Asymmetric ground state spin configuration of transverse domain wall on symmetrically notched ferromagnetic nanowires, Appl. Phys. Lett. 97 (2010) 022511.
[13] L. O'Brien, D. Petit, E.R. Lewis, R.P. Cowburn, D.E. Read, J. Sampaio, H.T. Zeng, A.V. Jausovec, Tunable remote pinning of domain walls in magnetic nanowires, Phys. Rev. Lett. 106 (2011) 087204.
[14] P. Gawroński, V. Zhukova, A. Zhukov, J. Gonzalez, Manipulation of domain propagation dynamics with the magnetostatic interaction in a pair of Fe-rich amorphous microwires, J. Appl. Phys. 114 (2013) 043903, doi:10.1063/1.4816271.
[15] V. Zhukova, J.M. Blanco, M. Ipatov, A. Zhukov, Magnetoelastic contribution in domain wall dynamics of amorphous microwires, Phys. B 407 (2012) 1450–1454, doi:10.1016/j.physb.2011.09.124.
[16] S.A. Baranov, V.S. Larin, A.V. Torcunov, Technology, preparation and properties of the cast glass-coated magnetic microwires, Crystals 7 (2017) 136, doi:10.3390/cryst7060136.
[17] H. Chiriac, S. Corodeanu, M. Lostun, G. Ababei, T.A. Óvári, Rapidly solidified amorphous nanowires, J. Appl. Phys. 107 (2010) 09A301.
[18] A. Zhukov, M. Ipatov, A. Talaat, J.M. Blanco, B. Hernando, L. Gonzalez-Legarreta, J.J. Suñol, V. Zhukova, Correlation of crystalline structure with magnetic and transport properties of glass-coated microwires, Crystals 7 (2017) 41.
[19] A.S. Antonov, V.T. Borisov, O.V. Borisov, A.F. Prokoshin, N.A. Usov, Residual quenching stresses in glass-coated amorphous ferromagnetic microwires, J. Phys. D Appl. Phys. 33 (2000) 1161–1168.
[20] H. Chiriac, T.A. Ovari, G. Pop, Internal stress distribution in glass-covered amorphous magnetic wires, Phys. Rev. B 42 (1995) 10105.
[21] H. Chiriac, T.A. Óvári, Switching field calculations in amorphous microwires with positive magnetostriction, J. Magn. Magn. Mater. 249/1-2 (2002) 141–145.
[22] P. Klein, R. Varga, G.A. Badini-Confalonieri, M. Vazquez, Study of the switching field in amorphous and nanocrystalline FeCoMoB microwire, IEEE Trans. Magn. 46 (2010) 357–360.
[23] M. Vázquez, D.X. Chen, The magnetization reversal process in amorphous wires, IEEE Trans. Magn. 31 (1995) 1229–1239.
[24] S. Corodeanu, H. Chiriac, T.A. Óvári, Accurate measurement of domain wall velocity in amorphous microwires, submicron wires and nanowires, Rev. Sci. Instrum. 82 (2011) 094701.
[25] R. Varga, K.L. García, M. Vázquez, A. Zhukov, P. Vojtanik, Switching field distribution in amorphous magnetic bistable microwires, Phys. Rev. B 70 (2004) 024401–024402.
[26] S.H. Yang, K.S. Ryu, S. Parkin, Domain-wall velocities of up to 750 m s^{-1} driven by exchange-coupling torque in synthetic antiferromagnets, Nat. Nanotechnol. 10 (2015) 221–226, doi:10.1038/nnano.2014.324.
[27] J. Yang, G.S.D. Beach, C. Knutson, J.L. Erskine, Magnetic domain-wall velocity enhancement induced by a transverse magnetic field, J. Magn. Magn. Mater. 397 (2016) 325–332.
[28] A. Zhukov, J.M. Blanco, M. Ipatov, V. Zhukova, Fast magnetization switching in thin wires: magnetoelastic and defects contributions, IEEE Sens. Lett. 11 (1) (2013) 170–176, doi:10.1166/sl.2013.2771.
[29] P. Corte-León, J.M. Blanco, V. Zhukova, M. Ipatov, J. Gonzalez, M. Churyukanova, S. Taskaev, A. Zhukov, Engineering of magnetic softness and domain wall dynamics of Fe-rich amorphous microwires by stress- induced magnetic anisotropy, Sci. Rep. 9 (2019) 12427, doi:10.1038/s41598-019-48755-4.
[30] D. Atkinson, D.S. Eastwood, L.K. Bogart, Controlling domain wall pinning in planar nanowires by selecting domain wall type and its application in a memory concept, Appl. Phys. Lett. 92 (2008) 022510.
[31] A. Kunz, Field induced domain wall collisions in thin magnetic nanowires, Appl. Phys. Lett. 94 (2009) 132502.
[32] A. Zhukov, J.M. Blanco, A. Chizhik, M. Ipatov, V. Rodionova, V. Zhukova, Manipulation of domain wall dynamics in amorphous microwires through domain wall collision, J. Appl. Phys. 114 (2013) 043910, doi:10.1063/1.4816560.
[33] A. Janutka, Externally driven collisions of domain walls in bistable systems near criticality, Phys. Rev. E 83 (2011) 056608.
[34] V. Zhukova, J.M. Blamco, P. Corte-León, M. Ipatov, M. Churyukanova, S. Taskaev, A. Zhukov, Grading the magnetic anisotropy and engineering the domain wall dysnamics in Fe-rich microwires by stress-annealing, Acta Mater. 155 (2018) 279–285.
[35] M. Vazquez, G.A. Basheed, G. Infante, R.P. Del Real, Trapping and injecting single domain walls in magnetic wire by local fields, Phys. Rev. Lett. 108 (2012) 037201.
[36] M. Ipatov, N.A. Usov, A. Zhukov, J. Gonzalez, Local nucleation fields of Fe-rich microwires and their dependence on applied stresses, Phys. B 403 (2008) 379–381.
[37] V. Zhukova, J.M. Blanco, M. Ipatov, J. Gonzalez, M. Churyukanova, A. Zhukov, Engineering of magnetic softness and giant magnetoimpedance effect in Fe-rich microwires by stress-annealing, Scr. Mater. 142 (2018) 10–14.
[38] P. Corte-Leon, V. Zhukova, J.M. Blanco, M. Ipatov, S. Taskaev, M. Churyukanova, J. Gonzalez, A. Zhukov, Engineering of magnetic properties and magnetoimpedance effect in Fe-rich microwires by reversible and irreversible stress-annealing anisotropy, J. Alloy. Compd. 855 (2021) 157460.
[39] N.L. Schryer, L.R. Walker, The motion of 180° domain walls in uniform dc magnetic fields, J. Appl. Phys. 45 (12) (1974) 5406–5421.
[40] J. Yang, C. Nistor, G.S.D. Beach, J.L. Erskine, Magnetic domain-wall velocity oscillations in permalloy nanowires, Phys. Rev. B 77 (2008) 014413.
[41] M. Churyukanova, V. Semenkova, S. Kaloshkin, E. Shuvaeva, S. Gudoshnikov, V. Zhukova, I. Shchetinin, A. Zhukov, Magnetostriction investigation of soft magnetic microwires, Phys. Status Solidi A 213 (2) (2016) 363–367, doi:10.1002/pssa.201532552.
[42] L. Gonzalez-Legarreta, P. Corte-Leon, V. Zhukova, M. Ipatov, J.M. Blanco, J. Gonzalez, A. Zhukov, Optimization of magnetic properties and GMI effect of thin Co-rich microwires for GMI microsensors, Sensors 20 (2020) 1558, doi:10.3390/s20061558.
[43] V. Zhukova, J.M. Blanco, M. Ipatov, M. Churyukanova, S. Taskaev, A. Zhukov, Tailoring of magnetoimpedance effect and magnetic softness of Fe-rich glass–coated microwires by stress- annealing, Sci. Rep. 8 (2018) 3202.
[44] K. Richter, R. Varga, G.A. Badini-Confalonieri, M. Vázquez, The effect of transverse field on fast domain wall dynamics in magnetic microwires, Appl.Phys. Lett. 96 (2010) 182507.
[45] A. Stupakiewicz, A. Chizhik, M. Tekielak, A. Zhukov, J. Gonzalez, A. Maziewski, Direct imaging of the magnetization reversal in microwires using all-MOKE microscopy, Rev. Sci. Instrum. 85 (2014) 103702, doi:10.1063/1.4896758.
[46] J.N. Nderu, M. Takajo, J. Yamasaki, F.B. Humphrey, Effect of stress on the bamboo domains and magnetization process of CoSiB amorphous wire, IEEE Trans. Magn. 34 (4) (1998) 1312–1314.
[47] V. Zhukova, J.M. Blanco, A. Chizhik, M. Ipatov, A. Zhukov, AC-current-induced magnetization switching in amorphous microwires, Front. Phys. 13 (2) (2018) 137501, doi:10.1007/s11467-017-0722-6.
[48] J.L. Tsai, H.T. Tzeng, B.F. Liu, Magnetic properties and microstructure of graded Fe/FePt films, J. Appl. Phys. 107 (2010) 113923.
[49] C.L. Zha, R.K. Dumas, Y.Y. Fang, V. Bonanni, J. Nogués, J. Åkerman, Continuously graded anisotropy in single $(Fe_{53}Pt_{47})_{100-x}Cu_x$ films, Appl. Phys. Lett. 97 (2010) 182504.
[50] R. Skomski, T.A. George, D.J. Sellmyer, Nucleation, and wall motion in graded media, J. Appl. Phys. 103 (2008) 07F531.
[51] A. Kunz, S.C. Reiff, Enhancing domain wall speed in nanowires with transverse magnetic fields, J. Appl. Phys. 103 (2008) 07D903.
[52] F. Beck, J.N. Rigue, M. Carara, The profile of the domain walls in amorphous glass-covered microwires, J. Magn. Magn. Mater. 435 (2017) 21–25.
[53] M. Kladivová, J. Ziman, J, Properties of a domain wall in a bi-stable magnetic microwire, J. Magn. Magn. Mater. 480 (2019) 193–198.
[54] S.A. Gudoshnikov, Y.B. Grebenshchikov, B.Y. Ljubimov, P.S. Palvanov, N.A. Usov, M. Ipatov, A. Zhukov, J. Gonzalez, Ground state magnetization distribution and

characteristic width of head to head domain wall in Fe-rich amorphous microwire, Phys. Status Solidi A 206 (4) (2009) 613–617.
[55] P.A. Ekstrom, A. Zhukov, Spatial structure of the head-to-head propagating domain wall in glass-covered FeSiB microwire, J. Phys. D Appl. Phys. 43 (2010) 205001.
[56] M. Kladivová, J. Ziman, Properties of a domain wall in a bi-stable magnetic microwire, J. Magn. Magn. Mater. 480 (2019) 193–198.
[57] L.V. Panina, M. Ipatov, V. Zhukova, A. Zhukov, Domain wall propagation in Fe-rich amorphous microwires, Phys, B 407 (2012) 1442–1445.
[58] F. Beck, J.N. Rigue, M. Carara, Effect of electric current on domain wall dynamics, IEEE Trans. Magn. 9 (8) (2013) 4699–4702.
[59] N.N. Orlova, V.S. Gornakov, A.S. Aronin, Role of internal stresses in the formation of magnetic structure and magnetic properties of iron-based glass coated microwires, J. Appl. Phys. 121 (2017) 205108, doi:10.1063/1.4984055.
[60] V. Zhukova, J.M. Blanco, M. Ipatov, A. Zhukov, Effect of transverse magnetic field on domain wall propagation inmagnetically bistable glass-coated amorphous microwires, J. Appl. Phys. 106 (2009) 113914.
[61] E. Berganza, M. Jaafar, C. Bran, J.A. Fernández-Roldán, O. Chubykalo-Fesenko, M. Vázquez, A. Asenjo, Multisegmented nanowires: a step towards the control of the domain wall configuration, Sci. Rep. 7 (2017) 11576.
[62] F.E. Luborsky, J.L. Walter, Magnetic anneal anisotropy in amorphous alloys, IEEE Trans. Magn. 13 (1977) 953–956 Mag.
[63] J. Haimovich, T. Jagielinski, T. Egami, Magnetic and structural effects of anelastic deformation of an amorphous alloy, J. Appl. Phys. 57 (1985) 3581–3583.
[64] M. Ohnuma, G. Herzer, P. Kozikowski, C. Polak, V. Budinsky, S. Koppoju, Structural anisotropy of amorphous alloys with creep-induced magnetic anisotropy, Acta Mater. 60 (3) (2012) 1278–1286.
[65] O. Ciubotariu, A. Semisalova, K. Lenz, M. Albrecht, Strain-induced perpendicular magnetic anisotropy and gilbert damping of $Tm_3Fe_5O_{12}$ thin films, Sci. Rep. 9 (2019) 17474, doi:10.1038/s41598-019-53255-6.
[66] A. Srivastava, K. Cole, A. Wadsworth, T. Burton, C. Mewes, T. Mewes, G.B. Thompson, R.D. Noebe, A.M. Leary, Broadband characterization of stress induced anisotropy in nanocomposite $Co_{74.6}Fe_{2.7}Mn_{2.7}Nb_4Si_2B_{14}$, J. Magn. Magn. Mater. 500 (2020) 166307.
[67] G. Infante, R. Varga, G.A. Badini-Confalonieri, M. Vázquez, Locally induced domain wall damping in a thin magnetic wire, Appl. Phys. Lett. 95 (2009) 012503.